COVID-19: A View from the Labor Market*

Joshua Bernstein

Alexander W. Richter Nathaniel A. Throckmorton

April 22, 2020

ABSTRACT

This paper examines the response of the U.S. labor market to a large and persistent job separation rate shock, motivated by the ongoing economic effects of the COVID-19 pandemic. We use nonlinear methods to analytically and numerically characterize the responses of vacancy creation and unemployment. Vacancies decline in response to the shock when firms expect persistent job destruction and the number of unemployed searching for work is low. Quantitatively, under our baseline forecast the unemployment rate peaks at 19.7%, 2 months after the shock, and takes 1 year to return to 5%. Relative to a scenario without the shock, unemployment uncertainty rises by a factor of 11. Nonlinear methods are crucial. In the linear economy, the unemployment rate "only" rises to 9.2%, vacancies increase, and uncertainty is unaffected. In both cases, the severity of the COVID-19 shock depends on the separation rate persistence.

Keywords: Unemployment Rate; Vacancies; Separation Rate; Pandemic; Nonlinear Solution
JEL Classifications: E24; E27; J63

*Bernstein, Department of Economics, Indiana University, 100 S. Woodlawn, Bloomington, IN 47405 (jmbernst@iu.edu); Richter, Research Department, Federal Reserve Bank of Dallas, 2200 N Pearl Street, Dallas, TX 75201 (alex.richter@dal.frb.org); Throckmorton, Department of Economics, William & Mary, P.O. Box 8795, Williamsburg, VA 23187 (nat@wm.edu). We thank Tyler Atkinson for useful discussions. The views in this paper are our own and do not necessarily reflect the views of the Federal Reserve Bank of Dallas or the Federal Reserve System.

1 INTRODUCTION

Beginning in mid-March 2020, U.S. initial unemployment claims sky-rocketed to an unprecedented level due to the COVID-19 pandemic and ensuing "stay-at-home" policies implemented throughout the country.[1] The spike in unemployment claims has already led to a significant increase in the unemployment rate and estimates indicate it will continue to rise and peak between 14.0% and 32.1% in 2020.[2] In light of this novel shock, it is crucial to examine what the labor market response might look like over the medium-term while tracing out the underlying mechanisms.

We use a nonlinear search and matching model similar to Hagedorn and Manovskii (2008) to examine the economy's response to a large positive shock to the job separation rate. The shock is designed to capture the sharp increase in initial unemployment claims due to COVID-19. Our analysis focuses on the short and medium-term dynamics of the unemployment rate and vacancies along the economy's response path to the shock. This exercise offers valuable insights into the mechanisms behind COVID-19's impact on the labor market, which is a key ingredient for any policy that seeks to alter the longer-run evolution of the labor market in the post-pandemic world.

We begin by analytically characterizing the response of vacancies to a separation rate shock. The shock affects vacancy creation through two distinct channels. First, a positive separation rate shock lowers the expected duration and hence the marginal benefit of a new job, which weakens the firm's incentives to post vacancies. Second, an increase in the separation rate eventually causes an increase in the number of unemployed workers searching for jobs. This increases the probability of filling a new vacancy, which all else equal encourages the firm to post new vacancies in equilibrium.

Our analytical approach uses second-order approximations to cleanly derive these effects. This shows the conditions under which the first effect dominates the second effect, causing vacancies to decrease in response to a positive separation rate shock. Intuitively, vacancies fall when the increase in number of unemployed workers searching for jobs is sufficiently small, so that the reduction in worker profitability dominates the increase in the likelihood of filling a new vacancy.

Furthermore, we use our second-order approximation to study how higher order moments respond to separation rate shocks. In particular, we show the conditional variance of future unemployment (i.e., uncertainty) increases in response to a positive separation rate shock. This result is driven by the convex response of equilibrium job creation (vacancies times the job-filling rate) to a separation rate shock. Intuitively, convexity implies a positive separation rate shock increases both

[1] In February 2020 there were $211{,}000$ initial unemployment claims on average, the lowest level since November 1969. For the week of March 15th, when the pandemic started to broadly affect the U.S., initial claims rose to 3.31 million. In total over the first month of the pandemic, unemployment claims increased by a staggering 22.03 million. For perspective, "only" 9.07 million claims were filed during the Great Recession from December 2007 to June 2009.

[2] On average, panelists from the April 2020 Blue Chip Economic Indicators survey estimated the peak U.S. unemployment rate in 2020 would reach 14.0%. An estimate from the Federal Reserve Bank of St. Louis found the unemployment rate could hit 32.1% in the second quarter (Faria-e-Castro, 2020a). Despite the wide range, either value would reflect the highest monthly unemployment rate on record. The previous peak was 10.8% in November 1982.

the conditional mean and conditional variance of future job creation, and therefore unemployment.

Our quantitative analysis is based on simulations of the nonlinear model. The severity of the COVID-19 shock depends on the separation rate persistence, which determines the speed of the recovery. In response to the shock in our baseline simulation, the unemployment rate peaks at 19.7%, 2 months after the shock, and takes 1 year to return to 5%. Furthermore, unemployment uncertainty increases by a factor of 11, relative to a scenario without the shock. We interpret these results as demonstrating the potentially large and long-lasting economic impact of the COVID-19 pandemic.

In line with our analytical insights, the large unemployment response is driven by a marked decline in vacancy creation by firms. This in turn is driven by a large reduction in the profitability of new matches that initially outweighs the increase in the number of unemployed workers searching for a job. When the separation rate declines, profitability increases, and vacancy creation recovers.

We emphasize the importance of using nonlinear methods by comparing the nonlinear responses to those from a linear version of the model. In the absence of higher-order effects, the unemployment rate increases to only 9.2%, well below current forecasts. Vacancies oddly increase on impact. The muted predictions occur because the linear model does not account for the interaction between the expected job separation rate and the expected job filling rate, which amplifies the equilibrium decline in the marginal benefit of posting a vacancy. These results demonstrate the important role that higher-order effects play in generating reasonable responses to a separation rate shock.

Related Literature There are two broad categories of the emerging literature that examines the economic effects of the COVID-19 pandemic. The first category uses the Markov-switching SIR (i.e., people are either susceptible to, infected by, or recovered from the disease) epidemiology model (Atkeson, 2020). For example, Alvarez et al. (2020) study optimal lockdowns that reduce fatalities while also minimizing the economic costs. In a similar model, Berger et al. (2020) also study the policies of disease testing and case-dependent quarantines. Eichenbaum et al. (2020) extend the model so the shock affects supply and demand and find the economic costs are 6 to 7 times larger. Alternatively, Jones et al. (2020) and Piguillem and Shi (2020) argue the congestion and limited capacity of the health care system is an important consideration for optimal policy.[3]

The second category of papers employ a New Keynesian and/or multi-sector model to analyze different policies. In a New Keynesian model, Fornaro and Wolf (2020) highlight how a negative supply shock can create a "doom loop" that disrupts supply and leads to a pessimism trap with low growth and high unemployment, where aggressive fiscal policy is needed to prevent economic stagnation. In a multi-sector nonlinear New Keynesian model, Faria-e-Castro (2020b) shows that the shutdown of contact-intensive service sectors can trigger a deep recession and then studies the

[3]Other papers examine the COVID-19 pandemic in a historical context. Jordà et al. (2020) compare the COVID-19 pandemic to past pandemics and wars and find longer-lasting economic effects of pandemics. Barro et al. (2020) study the 1918 pandemic and argue the effects on GDP and consumption are an upper bound for the COVID-19 pandemic.

effects of recent monetary and fiscal policies. Furthermore, Guerrieri et al. (2020) find an important role for incomplete markets where firms shutdown and exit in response to aggregate supply shocks, which has important policy implications for fiscal multipliers and preventing firms from exiting.

Our paper complements the existing literature in an important way. We examine the effects of the COVID-19 pandemic through the lens of the labor market, which is a crucial element of the pandemic's transmission to the economy. To facilitate our analysis, we modify a textbook search and matching model. Rather than shocking productivity, as others have done, the unprecedented increase in initial unemployment claims is interpreted as a once-in-a-century job separation shock.

We also contribute to the literature that uses nonlinear methods to analyze search and matching models. To our knowledge, we are the first to provide nonlinear analytical characterizations of key variables such as vacancy creation, and higher order moments such as unemployment uncertainty. These results are helpful in understanding the significant nonlinearities we numerically uncover. Quantitatively, we build on Petrosky-Nadeau and Zhang (2017) and Petrosky-Nadeau et al. (2018), who study the nonlinear responses to productivity shocks, by focusing on separation rate shocks.

The paper proceeds as follows. Section 2 introduces the economic environment, Section 3 contains our analytical results, and Section 4 presents our quantitative results. Section 5 concludes.

2 ENVIRONMENT

We situate our analysis in a textbook, infinite horizon search and matching model similar to Hagedorn and Manovskii (2008). A representative household and a representative firm interact in a frictional labor market. In each period, members of the household are either employed or unemployed. The mass of household members is normalized to unity so the number employed equals the aggregate employment rate. Employed workers receive a wage determined by Nash Bargaining.

Search and Matching At the beginning of period t, the employment rate is n_{t-1}. A fraction s_t of employed workers then lose their jobs, where s_t is the exogenous separation rate, which follows

$$\ln s_{t+1} = (1-\rho_s)\ln \bar{s} + \rho_s \ln s_t + \sigma_s \varepsilon_{t+1},\ \varepsilon \sim \mathbb{N}(0,1). \tag{1}$$

Therefore, the total number of unemployed people searching for work in period t is given by

$$u_t^s = 1 - n_{t-1} + s_t n_{t-1}. \tag{2}$$

If firms post v_t vacancies, then the number of new matches is determined by the following function

$$m_t = u_t^s v_t / ((u_t^s)^\iota + v_t^\iota)^{1/\iota}, \tag{3}$$

where $\iota > 0$ determines the curvature of the function. Define $\theta_t \equiv v_t/u_t^s$ as labor market tightness from the firm's perspective. Then the job finding rate, f_t, and job filling rate, q_t, are given by

$$f_t = m_t/u_t^s = 1/(1+\theta_t^{-\iota})^{1/\iota}, \tag{4}$$

$$q_t = m_t/v_t = 1/(1+\theta_t^{\iota})^{1/\iota}. \tag{5}$$

The specification of the matching function follows Den Haan et al. (2000). Compared to a Cobb-Douglas specification, (3) ensures the job-filling and job-finding rates remain between 0 and 1. This distinction is particularly important when shocks drive the economy far away from steady state.

Following Blanchard and Galí (2010), we assume newly matched workers begin employment in the same period they are matched with a firm, so aggregate employment evolves according to

$$n_t = (1-s_t)n_{t-1} + q_t v_t. \tag{6}$$

The unemployment rate, u_t, is includes anyone who is not matched in period t, so

$$u_t \equiv u_t^s - m_t = 1 - n_t. \tag{7}$$

Firms A representative firm produces the final good by operating a constant returns to scale technology that uses labor as the only input. Vacancies and labor demand $\{v_t, n_t\}$ are chosen to maximize the present value of dividends, $V_t = n_t - w_t n_t - \kappa v_t + \beta E_t[V_{t+1}]$, subject to (6) and $v_t \geq 0$, where $\kappa > 0$ is the vacancy posting cost, w is the wage rate, and E_t is the mathematical expectation operator condition on information at time t. Letting λ_t denote the Lagrange multiplier on the non-negativity constraint and $S_{n,t}$ the Lagrange multiplier on (6), the optimality conditions are given by

$$S_{n,t} = \kappa/q_t - \lambda_t, \tag{8}$$

$$S_{n,t} = 1 - w_t + \beta E_t[(1-s_{t+1})S_{n,t+1}], \tag{9}$$

which imply

$$\kappa/q_t - \lambda_t = 1 - w_t + \beta E_t[(1-s_{t+1})(\kappa/q_{t+1} - \lambda_{t+1})]. \tag{10}$$

This condition states that the marginal cost of posting an additional vacancy at time t equals the marginal benefit of an additional worker. The benefit includes the time-t profit from the new match plus the discounted expected value of the worker, net of the separations that occur at time $t+1$. Also note that $S_{n,t}$ is interpreted as the marginal surplus value of a new match to the firm at time t.

Households Given paths for employment and unemployment, the household maximizes lifetime utility, $J_t = c_t + \beta E_t J_{t+1}$, subject to $c_t = w_t n_t + b u_t - \tau_t + d_t$, where b is the unemployment benefit, τ_t is a lump-sum tax, and d_t is dividends from ownership of the firm. Applying the envelope

theorem, we obtain the marginal utilities of employment and unemployment given by

$$J_{n,t} = w_t + \beta E_t[((1 - s_{t+1}(1 - f_{t+1}))J_{n,t+1} + s_{t+1}(1 - f_{t+1})J_{u,t+1})],$$
$$J_{u,t} = b + \beta E_t[(f_{t+1}J_{n,t+1} + (1 - f_{t+1})J_{u,t+1})].$$

Hence, the marginal surplus of employment over unemployment is given by

$$J_{n,t} - J_{u,t} = w_t - b + \beta E_t[(1 - f_{t+1})(1 - s_{t+1})(J_{n,t+1} - J_{u,t+1})]. \tag{11}$$

Wage Rate Wages are determined via Nash Bargaining between an employed worker and the firm. The total surplus of a match is $\Lambda_t = (J_{n,t} - J_{u,t}) + S_{n,t}$. The equilibrium wage rate maximizes $(J_{n,t} - J_{u,t})^{\eta}(S_{n,t})^{1-\eta}$, where $\eta \in [0, 1]$ is the household's bargaining weight. Optimality implies

$$J_{n,t} - J_{u,t} = \eta\Lambda_t \tag{12}$$

or, equivalently,

$$S_{n,t} = (1 - \eta)\Lambda_t. \tag{13}$$

To derive the equilibrium wage rate, first plug (11) into (12) to obtain

$$\eta\Lambda_t = w_t - b + \eta\beta E_t[(1 - s_{t+1})(1 - f_{t+1})\Lambda_{t+1}]. \tag{14}$$

Then plug (9) in (13) and combine with (14) to obtain

$$w_t = \eta(1 + \kappa\beta E_t[(1 - s_{t+1})\theta_{t+1}]) + (1 - \eta)b. \tag{15}$$

The wage rate in period t is a weighted average of the representative firm's value of a new match and the representative household's cost of working. The firm's value of a new worker includes the additional output produced plus the discounted expected value of the foregone vacancy cost net of separations that occur in period $t + 1$. The household's cost is the foregone unemployment benefit.

Equilibrium Given the government budget constraint, $\tau_t = bu_t$, the resource constraint is given by

$$c_t + \kappa v_t = n_t. \tag{16}$$

A competitive equilibrium is sequences of quantities $\{c_t, n_t, u_t, u_t^s, v_t, q_t\}_{t=0}^{\infty}$, prices $\{w_t\}_{t=0}^{\infty}$, and exogenous variables $\{s_t\}_{t=1}^{\infty}$ that satisfy (1), (2), (5)-(7), (10), (15), and (16) given states $\{n_{-1}, s_0\}$.

3 ANALYTICAL RESULTS

The dynamics of the standard search and matching model are driven by the representative firm's vacancy creation decision. In our context, this choice is crucial in determining the response of the

economy, in particular the unemployment rate, to the separation rate shock that occurs due to the pandemic. This section combines simplifying assumptions with approximation techniques to shed light on the determinants of vacancy creation at both the micro and macro levels. We also discuss how vacancy creation drives endogenous fluctuations in uncertainty about the unemployment rate.

3.1 DRIVERS OF AGGREGATE VACANCY CREATION

Substituting (15) into (10) implies[4]

$$\kappa/q_t = (1-\eta)(1-b) + \beta E_t[(1-s_{t+1})(1-\eta\theta_{t+1}q_{t+1})\kappa/q_{t+1}].$$

In our quantitative exercise, we set the bargaining weight close to zero following Hagedorn and Manovskii (2008). Therefore, in order to simplify the qualitative analysis, we set $\eta = 0$ to obtain

$$\underbrace{\kappa/q_t}_{mc_t} = \underbrace{1-b}_{mb_t} + \underbrace{\beta E_t[(1-s_{t+1})\kappa/q_{t+1}]}_{mb_{t+1}}, \tag{17}$$

which has a simple microeconomic interpretation. The left-hand side is the marginal cost of posting a new vacancy—the flow cost of maintaining the posting multiplied by its expected duration. The right-hand side captures the static and dynamic marginal benefits of a new vacancy. The static benefit is the profit flow from a new match. The dynamic benefit captures the fact that, conditional on the match surviving, the firm saves the marginal cost of posting a new vacancy in period $t+1$.

Total vacancies are given by $v_t = \theta_t(1-(1-s_t)n_{t-1})$. Using (5) to substitute for θ, we obtain

$$v_t = \left(\kappa^{-\iota}(\kappa/q_t)^{\iota} - 1\right)^{1/\iota}(1-(1-s_t)n_{t-1}), \tag{18}$$

which shows vacancies can be decomposed into two components. The first component is driven by microeconomic considerations and is summarized by the firm's marginal cost of vacancy creation. All else equal, a higher marginal cost indicates the firm is creating more vacancies in equilibrium. Greater vacancy posting drives down the job-filling rate and hence raises the firm's marginal cost.

The second component is driven by the macroeconomic nature of the matching function. Recall that $u_t^s = 1-(1-s_t)n_{t-1}$ is the number of unemployed workers searching for jobs in period t. All else equal, when u_t^s is higher, more matches are created and the job-filling rate increases. This drives down the marginal cost of vacancy creation and results in an increase in vacancies created.

To understand how vacancies respond to separation rate shocks, we need to examine how each component responds. The second component increases in response to a positive separation rate shock. The higher separation rate causes u_t^s to rise, which *ceteris paribus* leads to higher vacancies.

Now consider how the first component responds to a positive separation rate shock. To facilitate the analysis, we use a second-order approximation of (17). Formally, let $\hat{x}_t \equiv \ln(x_t/x)$ denote the

[4]For tractability, we assume the constraint $v_t \geq 0$ never binds when deriving our analytical results. Numerically, the constraint only binds at extreme points in the state space, which we do not encounter in our quantitative exercise.

log deviation of a variable x_t from its deterministic steady-state value. We look for a solution where

$$\hat{q}_t = \phi_{q,1}\hat{s}_t + \tfrac{1}{2}\phi_{q,2}\hat{s}_t^2$$

for some coefficients $\phi_{q,1}$ and $\phi_{q,2}$.[5] The firm's marginal cost, $mc_t = \kappa/q_t$, is then approximated by

$$\hat{mc}_t = -\phi_{q,1}\hat{s}_t - \tfrac{1}{2}\phi_{q,2}\hat{s}_t^2.$$

Lemma 1. *Suppose* $\hat{q}_t = \phi_{q,1}\hat{s}_t + \frac{1}{2}\phi_{q,2}\hat{s}_t^2$ *solves* (17). *Then* $\phi_{q,1} > 0$ *and* $\phi_{q,2} > 0$.

Given the approximation to the vacancy creation equation, (17), this result says the job-filling rate is increasing and convex in the separation rate $\hat{s}_t$, while the marginal cost is decreasing and concave. We can also trace out the relation between $\hat{mc}_t$ and $\hat{s}_t$ by revisiting (17). Consider a positive and persistent shock to the separation rate, which causes both $\hat{s}_t$ and $E_t\hat{s}_{t+1}$ to increase. To a first order, the increase in $E_t\hat{s}_{t+1}$ lowers the dynamic benefit of posting a vacancy in period t since there is a larger chance that it gets destroyed in period $t+1$. In response, the firm chooses to post fewer vacancies, the job-filling rate increases, and the marginal cost of vacancy creation falls.[6]

To see the concavity, note that when $E_t\hat{s}_{t+1}$ increases, the future job-filling rate also increases. As a result, the future marginal cost of a vacancy falls, which exacerbates the reduction in the future marginal benefit of creating a vacancy in period t. The second-order interaction of these effects amplifies the equilibrium decline in the marginal cost of a vacancy in period t. Hence the drop in the firm's marginal cost is larger when accounting for second-order effects of separation rate shocks.

The response of vacancies to a separation rate shock is determined by two opposing forces. One, a positive shock lowers vacancy creation via the marginal cost channel—the future marginal benefit of a vacancy declines so firms create fewer vacancies. Two, a positive shock increases the number of unemployed workers searching for a job, which causes the job-filling rate and vacancies to increase. To formalize the effects of these channels, we derive a second order approximation of (18) in terms of $\hat{s}_t$ and $\hat{n}_{t-1}$, since vacancies directly depend on the endogenous state variable n_{t-1}.

Proposition 1. *Suppose* $\hat{q}_t = \phi_{q,1}\hat{s}_t + \frac{1}{2}\phi_{q,2}\hat{s}_t^2$ *solves* (17). *Then*

$$\hat{v}_t = \phi_{v,1}(\hat{n}_{t-1})\hat{s}_t + \tfrac{1}{2}\phi_{v,2}\hat{s}_t^2 + \psi_{v,1}\hat{n}_{t-1} + \tfrac{1}{2}\psi_{v,2}\hat{n}_{t-1}^2,$$

where $\phi_{v,1}(\hat{n})$ *is an affine function and all coefficients depend only on the deterministic steady state.*

In order to highlight how the marginal cost of vacancy creation and the number of unemployed workers searching for jobs create opposing effects of separation rate shocks on vacancy creation, it

[5] In general, we would approximate a function $q_t = q(s_t, n_{t-1})$ that also depends on the endogenous state variable. However, it turns out the dependence of q_t on n_{t-1} is numerically negligible compared to its dependence on s_t. Therefore, we streamline the analysis by restricting attention to an approximate solution in which q_t only depends on s_t.

[6] Appendix A defines the coefficients and provides detailed proofs of each lemma and proposition in this section.

is sufficient to focus on the function $\phi_{v,1}(\hat{n})$ in the first term of Proposition 1. Appendix A shows

$$\phi_{v,1}(\hat{n}_{t-1}) = \bar{f}(1 + \hat{n}_{t-1}/\bar{u}^s) - \phi_{q,1}/(1 - \bar{q}^\iota),$$

where a bar denotes a steady-state value. The first term in this expression captures the positive effect stemming a larger number of unemployed workers searching for jobs. It is increasing in the employment rate at the start of the period, $\hat{n}_{t-1}$. All else equal, higher employment results in a larger number of newly searching unemployed workers when the separation shock hits. The second term captures the marginal cost channel. All else equal, this expression shows the marginal cost channel will dominate when $\hat{n}_{t-1}$ is sufficiently small. In this case, the reduction in marginal cost driven by a fall in the future marginal benefit of a vacancy dominates the rise in the job-filling rate.

3.2 UNEMPLOYMENT UNCERTAINTY An advantage of our nonlinear approach is that we can study how shocks to the first moments of exogenous variables induce changes in the higher order moments of endogenous variables. Given our application, we focus on the uncertainty surrounding the unemployment rate, which we measure as the expected volatility of the 1-period ahead forecast error following Plante et al. (2018). Specifically, for a generic variable x, uncertainty is given by

$$\mathcal{U}^x_{t,t+1} = \sqrt{E_t[(x_{t+1} - E_t[x_{t+1}])^2]}.$$

The same definition is also used in recent empirical work on uncertainty (e.g., Jurado et al. 2015).

Applying this definition to the unemployment rate, $u_t = 1 - (1 - s_t)n_{t-1} - q_t v_t$, together with our approximations for the job-filling rate and vacancies, yields the following expression for $\mathcal{U}^u_{t,t+1}$.

Lemma 2. *If Lemma 1 and Proposition 1 hold, unemployment uncertainty is given by*

$$\mathcal{U}^u_{t,t+1} = (\bar{q}\bar{v}(\phi_{q,1} + \phi_{v,1}(\hat{n}_{t-1}) - 1 + (\phi_{q,2} + \phi^2_{q,1} + \phi_{v,2} + \phi_{v,1}(\hat{n}_{t-1})^2 - 1)\rho_s\hat{s}_t))\sigma_s.$$

The more $\hat{q}_{t+1}$ and $\hat{v}_{t+1}$ respond to $\hat{s}_{t+1}$, the larger is $\phi_{q,1} + \phi_{v,1}(\hat{n}_{t-1}) - 1 > 0$, and the larger is the conditional variance of u_{t+1}. Beyond these first-order considerations, Lemma 2 also shows that a shock to the separation rate in period t affects uncertainty about period $t+1$. In other words, first moment shocks to an exogenous variable affect the second moments of endogenous variables.

Proposition 2. *Suppose Lemma 2 holds. Then*

$$d\mathcal{U}^u_{t,t+1}/d\hat{s}_t = \bar{q}\bar{v}(\phi_{q,2} + \phi^2_{q,1} + \phi_{v,2} + \phi_{v,1}(\hat{n}_{t-1})^2 - 1)\rho_s\sigma_s.$$

To streamline the exposition, we restrict our attention to the case in which $d\mathcal{U}^u_{t,t+1}/d\hat{s}_t > 0$, so unemployment uncertainty is increasing in the current separation rate. We focus on this particular case because it is the most quantitatively relevant. Proposition 2 shows that this occurs when vacancies and the job-filling rate are sufficiently convex in the separation rate so that $\phi_{q,2} + \phi_{v,2} - 1 > 0$.

Why does the convexity of vacancies and the job-filling rate result in a positive response of unemployment uncertainty to separation rate shocks? Consider the impact of a positive separation rate shock in period t on the conditional distributions of $\hat{s}_{t+1}$, $\hat{q}_{t+1}$, and $\hat{v}_{t+1}$. While the mean of the conditional distribution of $\hat{s}_{t+1}$ increases, the conditional variance is unaffected since the shocks are exogenous. In contrast, the convexity of $\hat{q}_{t+1}$ and $\hat{v}_{t+1}$ with respect to $\hat{s}_{t+1}$ implies the increase in the conditional mean of $\hat{s}_{t+1}$ increases their conditional means and conditional variances. As a result, uncertainty about u_{t+1} increases in response to a positive separation rate shock in period t.

4 QUANTITATIVE ANALYSIS

In this section, we present our main numerical exercise and study the economy's response to a large positive separation rate shock. We view this exercise as informative of how frictions in the U.S. labor market will affect the response of unemployment to a large increase in job separations.

Subjective Discount Factor	β	0.9983	Vacancy Posting Cost	κ	0.615
Nash Bargaining Weight	η	0.052	Average Separation Rate	$\bar{s}$	0.035
Unemployment Benefit	b	0.955	Separation Rate Persistence	ρ_s	0.7071
Matching Function Curvature	ι	1.27	Separation Rate Standard Deviation	σ_s	0.3533

Table 1: Baseline parameter values.

4.1 CALIBRATION

Table 1 summarizes our baseline parameter values. A period in the model corresponds to 1 month. The subjective discount factor implies an annual real interest rate of 2%. The household's bargaining weight, η, and flow value of unemployment, b, are set to the values in Hagedorn and Manovskii (2008). The curvature in the matching function, ι, is consistent with the value in Den Haan et al. (2000). The average separation rate, $\bar{s}$, is 0.035, which is the average in the Job Openings and Labor Turnover Survey (JOLTS) since the series began in 2001. The vacancy cost, κ, implies an average unemployment rate of 6%, which equals the JOLTS sample average.

We calibrate the parameters of the exogenous separation rate process, (1), to reflect the effects of the COVID-19 pandemic. The baseline persistence of the process is based on a half-life of 2 months, but we also show the results with half-lives of 1 and 3 months to consider different recoveries. The low persistence captures that the temporary increase in separations is likely to quickly decline as state governments lift "stay-at-home" orders. We set the shock standard deviation so a COVID-19-type pandemic occurs once every 100 years, since the COVID-19 pandemic is widely considered the worst public health crisis since the 1918 influenza pandemic about 100 years ago.

The size of the COVID-19 shock is calibrated to unemployment claims data since the onset of the pandemic. From March 15-April 11, 2020, initial unemployment claims increased $22{,}034{,}000$. In February 2020, there were $5{,}560{,}000$ total separations, of which $1{,}755{,}000$ were either layoffs or

discharges, and 152,487,000 people employed. These values equate to a 3.7% separation rate. Using the increase in initial unemployment claims data over the last month as a proxy for the increase in layoffs, we estimate the first month of the pandemic will increase the separation rate to 17.0% $(100\times(3{,}805+22{,}034)/152{,}487)$, a staggering 13.3 percentage point increase from February 2020.

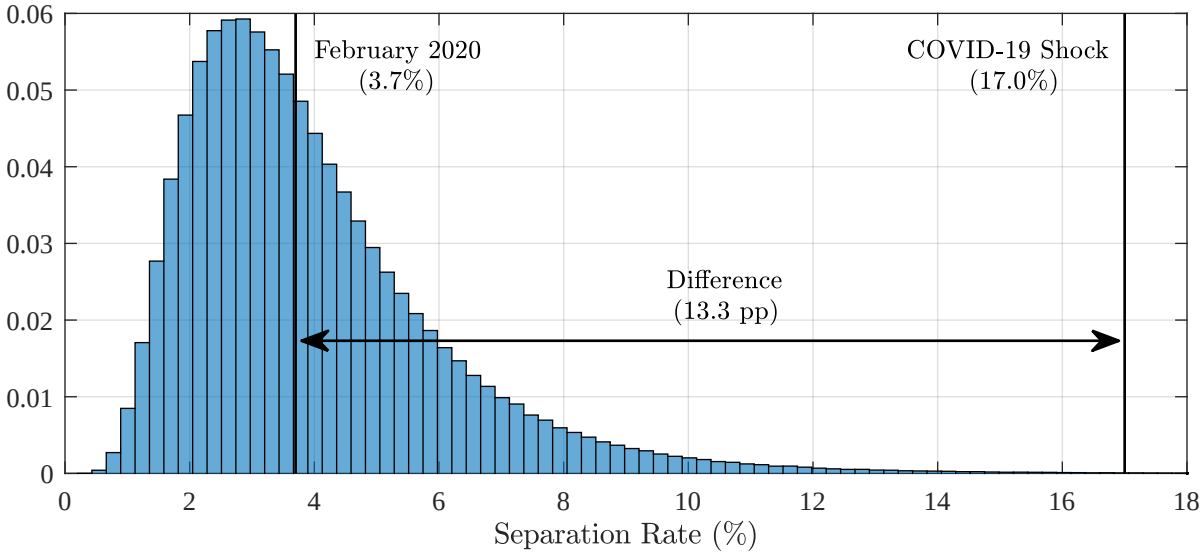

Figure 1: Separation rate distribution in our model.

Based on this calibration, Figure 1 plots the separation rate distribution from the model, which is asymmetric due to the log normality of the exogenous process. The COVID-19 shock appears far in the right tail of the distribution, reflecting that disruptions to the labor market of this magnitude are very rare and only affect the tail of the distribution of the household's expectations in the model.

4.2 SOLUTION METHODS We compare the predictions of our model using both the log-linear and fully nonlinear solutions. The linear version is solved using Sims's (2002) `gensys` algorithm. Using the linear solution as an initial conjecture, we solve the nonlinear model with the policy function iteration algorithm described in Richter et al. (2014), which is based on the theoretical work on monotone operators in Coleman (1991). Each iteration, the algorithm minimizes the Euler equation errors on every node in the discretized state space. It then computes the maximum distance between the policy functions on any node and iterates until that distance falls below the tolerance criterion. We approximate the continuous separation rate processes with an N-state Markov chain following Rouwenhorst (1995) and use piecewise linear interpolation to calculate the period-$t+1$ policy functions.[7] To ensure that v_t does not violate the non-negativity constraint, we introduce an auxiliary variable, μ_t, that is continuous in the state of the economy following Garcia and Zangwill (1981). See Appendix B for a detailed description of the nonlinear algorithm.

[7] Petrosky-Nadeau and Zhang (2017) show the Rouwenhorst method is crucial to accurately capture nonlinearities.

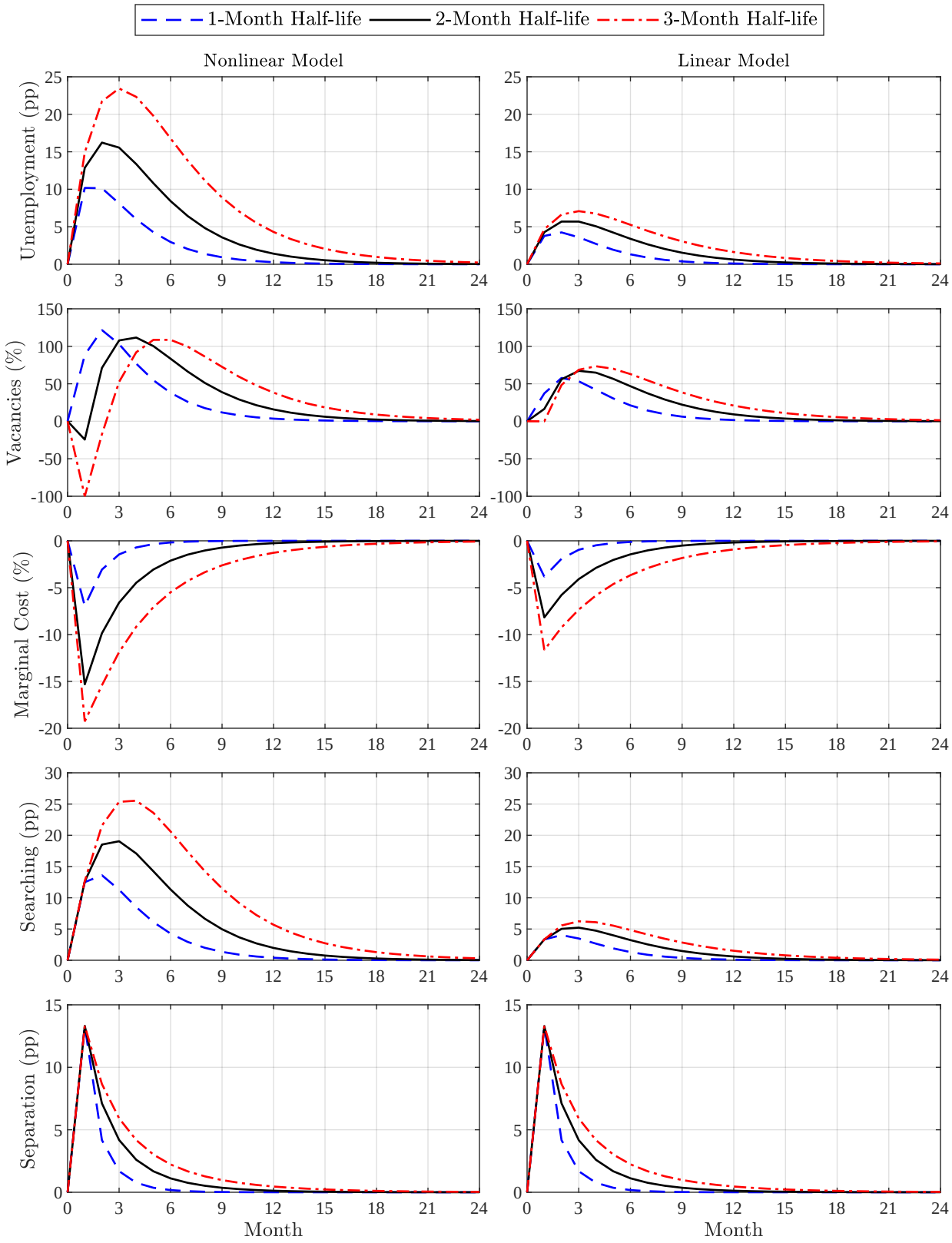

Figure 2: Impulse responses to a COVID-19 separation rate shock in deviations from a baseline simulation without the shock. Each simulation is initialized at a 3.5% unemployment rate, the rate from February 2020.

4.3 IMPULSE RESPONSES Figure 2 plots generalized impulse response functions (GIRFs) of key macroeconomic variables to the COVID-19 shock using the nonlinear solution to the model and compares them to traditional impulse responses using the linear solution. To compute a GIRF, we follow the procedure in Koop et al. (1996). We first calculate the mean path from $10{,}000$ simulations of the nonlinear model, conditional on random shocks in every quarter. We then calculate a second mean from another set of $10{,}000$ simulations, but this time the shock in the first quarter is replaced with the COVID-19 shock. The GIRF reports the difference between two mean paths. All of the simulations are initialized at a 3.5% unemployment rate, the rate from February 2020.

We begin by focusing on the solid-black curves in the left panel, which plot the responses to the baseline shock conditional on the nonlinear solution and our baseline calibration. There has been much speculation that the COVID-19 shock will result in a substantial increase in unemployment, as workers are laid-off or furloughed in response to virus-containment precautions. Our model is consistent with this prediction. Unemployment peaks at 19.7%, 16.2 percentage points above the rate in February 2020 and 2 months after the start of the pandemic. Furthermore, the model shows it takes 1 year for the unemployment rate to return to 5%. The large increase in separations caused by COVID-19 has immediate and medium-term implications for the health of the labor market.

As we emphasized in the analytical section, the response of unemployment is driven by the dynamics of vacancy creation, which is plotted in the second graph. In response to the shock, the level of vacancies plummets on impact, before increasing and decaying back to its pre-shock level.

To understand the non-monotonic dynamics of vacancy creation, we rely on our analytical results together with the third and forth panels of Figure 2, which show the responses of the two components of vacancy creation: marginal cost and the number of unemployed workers searching for jobs. In line with our analytical approximations, the marginal cost of vacancy creation drops in response to the shock, while the number of searching workers increases before decaying back to its pre-shock level. The fact that vacancies initially fall indicates that the drop in marginal cost dominates the rise in searching workers. Intuitively, the large and persistent increase in separations causes a severe decline in the marginal benefit of vacancy creation since firms do not expect new matches to last. Therefore, they initially cut back on vacancy creation. As the separation rate declines, however, the returns to vacancy creation increase, causing firms to create more vacancies.

There has been much debate over the severity of the job separations caused by COVID-19. In our model, severity is captured by the persistence parameter ρ_s. To analyze the effects of persistence, we compare the solid-black curves to the dashed-blue and dotted-red curves, which plot the responses to a shock with an equal magnitude but half-lives of 1 and 3 months, respectively. Lower persistence results in a smaller response of unemployment that peaks at "only" 13.7%, 1 month after the shock. The higher persistence leads to an alarming 26.9% unemployment rate, 3 months after the shock. Furthermore, the half-life affects when the economy normalizes. The unemployment

rate returns to 5% after 8 months under a 1-month half-life and 17 months under a 3-month half-life.

The response of the unemployment rate is driven the by response of vacancies. With a 3-month half-life, there is a larger decline in vacancies relative to the baseline calibration. With a 1-month half-life, vacancies significantly increase on impact. Intuitively, the persistence of the shock affects the marginal benefit of vacancy creation. With a lower persistence, the marginal benefit of vacancy creation does not fall as much on impact, as captured by the muted response of marginal cost. As a consequence, the response of vacancies is driven by the increase in unemployed workers searching for a job, which generates a higher job-filling rate and causes firms to post additional vacancies.

Interestingly, adding the unemployment rate responses to the initial unemployment rate of 3.5% results in a 13.7%-26.9% range of peak unemployment in second quarter 2020, which aligns with the range of forecasts mentioned in Section 1. This suggests the persistence of job separations caused by COVID-19 is a driving factor behind the uncertainty in the unemployment projections.

4.4 THE IMPORTANCE OF NONLINEARITIES Our analytical and numerical exercises examine nonlinear responses of the macroeconomy to separation rate shocks. To demonstrate the value of capturing these nonlinearities, we plot impulse responses using the log-linear solution in the right-hand panels of Figure 2. Using linear solution methods, we find much smaller responses of all variables to the COVID-19 shock, even though its underlying magnitude is unprecedented. Unemployment increases but by at most 7.1 percentage points, which is well below the expectations of most forecasters and policymakers. This makes sense, since linear solutions shut down higher-order amplification mechanisms by construction. For example, the response of the marginal cost is no longer concave, so the effect of separation rate shocks is simply proportional to the size of the shock.

In addition to generating smaller responses, the linear solution predicts that vacancies rise in response to the shock due to the rise in unemployed searching. This forecast is likely to be qualitatively counterfactual and is inconsistent with the existing evidence for the response of vacancies to separation rate shocks (Shimer, 2005). To see why the qualitative response of vacancies changes, consider the linear vacancy equation (dropping second order terms from Proposition 1), given by

$$\hat{v}_t = (\bar{f} - \phi_{q,1}/(1-\bar{q}^{\iota}))\hat{s}_t - \bar{n}(1-\bar{s})\hat{n}_{t-1}/\bar{u}^{s}.$$

The response of vacancies to the separation rate shock balances two opposing forces: a decrease driven by the decline in the marginal benefit (and hence marginal cost) of vacancy creation and an increase in vacancies driven by more searching workers. The numerical response of vacancies indicates that, using our standard calibration, the marginal cost channel is weak, and the coefficient on $\hat{s}_t$ is approximately zero. Therefore, the first-order response of vacancies is entirely driven by the dynamics of employment. This result also highlights further the importance of accounting for nonlinearities, which qualitatively affect the response of vacancy creation to the separation rate shock.

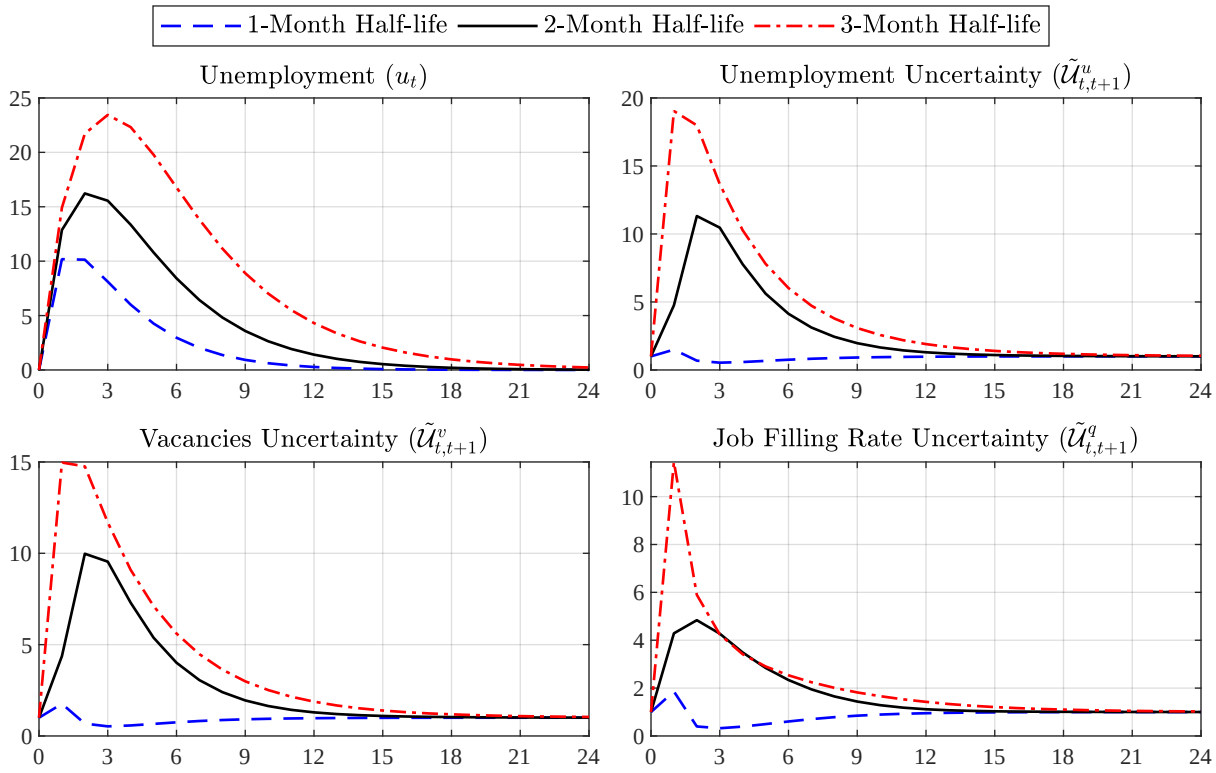

Figure 3: Impulse responses to a COVID-19 shock. Uncertainty is shown relative to the baseline simulation without the shock. Each simulation is initialized at a 3.5% unemployment rate, the rate from February 2020.

4.5 ENDOGENOUS UNCERTAINTY We now turn to examining the quantitative response of uncertainty to the COVID-19 pandemic. The top row of Figure 3 shows the response of the unemployment rate and its uncertainty over the next month to the separation rate shock. The uncertainty response is reported as a ratio relative to a baseline simulation without the shock, $\tilde{\mathcal{U}}^x_{t,t+1}$. Following the shock, $\tilde{\mathcal{U}}^u_{t,t+1}$ increases to 11, so uncertainty is 11 times larger than in the baseline simulation.

In the economy without the separation rate shock, unemployment uncertainty is only 0.05 percentage points. Given an actual unemployment rate of 3.5% (as reported in February 2020), this implies there is a 95% chance that the 1-Month ahead unemployment rate forecast is between 3.4% and 3.6%. In contrast, when the separation rate shock hits the economy, $\mathcal{U}^u_{t,t+1}$ increases to 0.6 percentage points. Given the realized unemployment rate of 19.7%, this level of uncertainty implies that unemployment rate forecasts are between 18.5% and 20.9% 95% of the time, which is a larger confidence interval than in the baseline simulation without the shock. This result indicates the increase in uncertainty in the data is likely a reaction to the first moment effects of the pandemic.

We investigate the sources of the increase in uncertainty by examining the changes in uncertainty for vacancy creation and the job-filling rate. These responses are shown in the bottom row of Figure 3. The results provide clear evidence that uncertainty increases for vacancies and the job-filling rate, reflecting the strong underlying convexities of their responses to separation rate shocks.

(a) Linear Model

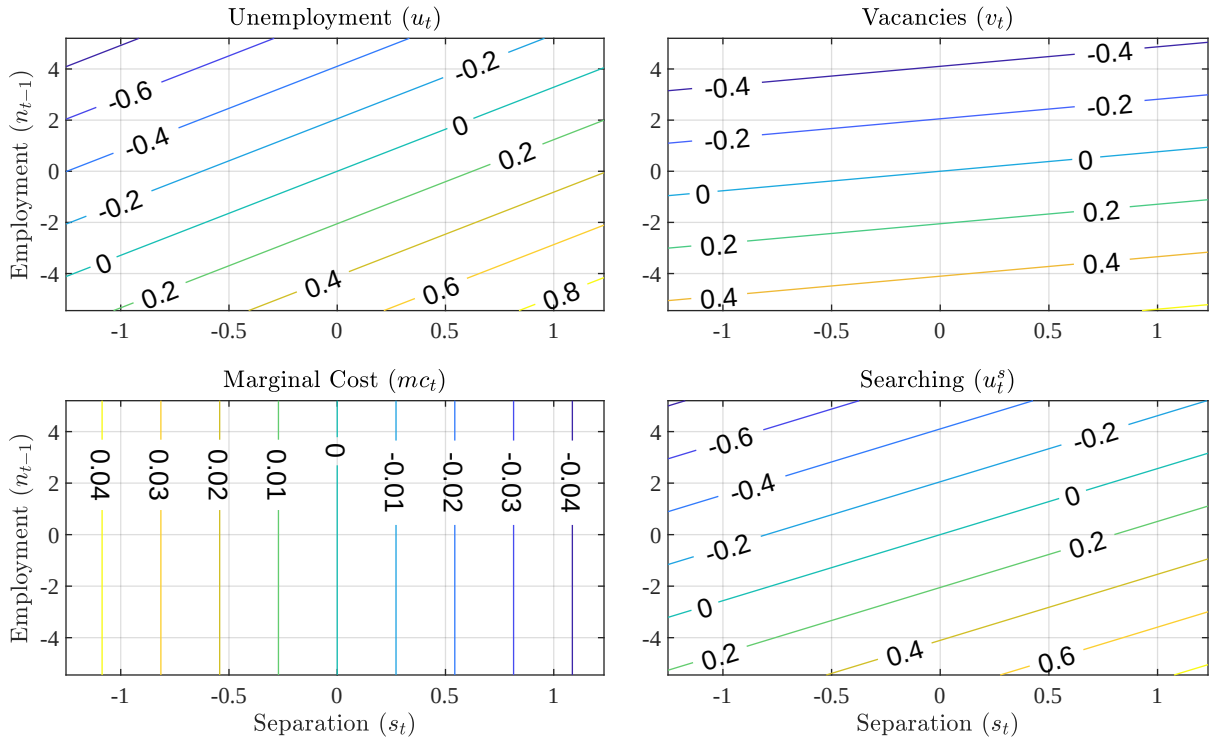

(b) Nonlinear Model

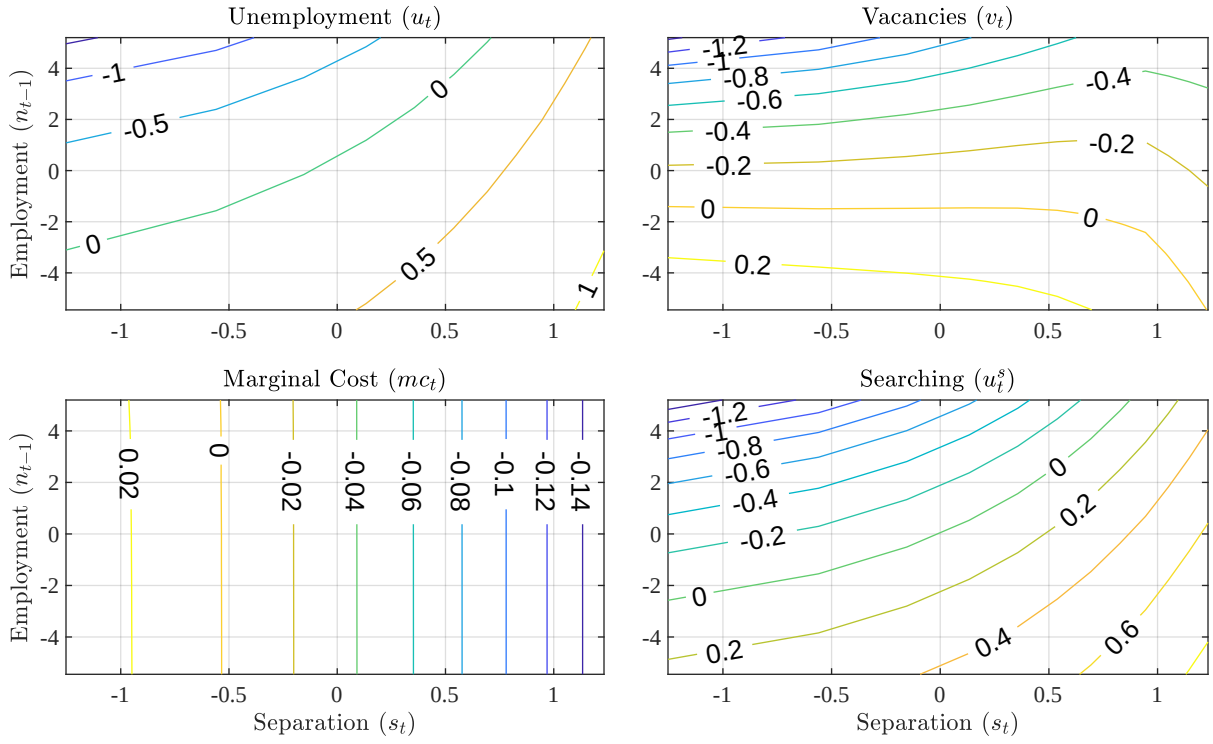

Figure 4: Policy function contour plots in deviations from the deterministic steady state. The employment grid is asymmetric to account for the COVID-19 shock but is shown symmetrically for illustrative purposes.

4.6 BEYOND THE COVID-19 SHOCK

While our main results are motivated by the ongoing pandemic crisis, we find it useful to distill some broader insights from our analysis. To this end, Figure 4 contains contour plots of the time-invariant policy functions for key macroeconomic variables. We compare the contours from the linear solution (top panel) to those obtained when we solve the model nonlinearly (bottom panel). All units on the axes and contours are in log deviations from the deterministic steady state to permit a direct comparison between the two approximations.

In both cases, an increase in the job separation rate causes unemployment to increase. However, the presence of higher-order amplification results in a stronger response of unemployment in the nonlinear model, as the impulse responses demonstrated. Comparing the vacancy plots highlights the stark effect of nonlinearities. To a first order, vacancies do not respond to the separation rate as the opposing effects of the shock cancel out. When we allow for higher-order terms, however, the response of vacancies becomes highly nonlinear. Depending on the employment state, n_{t-1}, a rise in the separation rate may cause vacancies to increase or decrease. Thus, there are states of the economy where the nonlinear model's predictions are qualitatively different than the linear model.

The discrepancy in the behavior of vacancies is in turn driven by qualitative differences in the responses of marginal cost. While marginal cost is generally unresponsive to employment, the linear model misses significant concavity in its response to the separation rate. This concavity plays a crucial role in ensuring that the falling marginal cost of hiring, which reduces vacancies, dominates the increase in vacancies caused by the increase in the number of unemployed searching.

5 CONCLUSION

This paper examines the response of the U.S. labor market to a large and persistent job separation rate shock, motivated by the ongoing economic effects of the COVID-19 pandemic. We use nonlinear methods to analytically and numerically characterize the responses of vacancy creation and unemployment. Vacancies decline in response to the shock when firms expect persistent job destruction and the number of unemployed searching for work is low. Quantitatively, under our baseline forecast the unemployment rate peaks at 19.7%, 2 months after the shock, and takes 1 year to return to 5%. In the linear economy, the unemployment rate "only" rises to 9.2% and vacancies increase. This shows nonlinearities are crucial to obtain reasonable predictions for the effects of COVID-19.

While this paper is motivated by the ongoing COVID-19 pandemic, we do not claim to provide a fully integrated analysis of the labor market in the presence of complex infection dynamics and containment policies. Instead, our contribution is to use a standard model to develop insights into the labor market's short and medium-term response to an important dimension of the pandemic's economic impact—a large and persistent increase in the job separation rate. Eventually, the health risks associated with the pandemic will subside and economic activity will resume. We believe our analysis will serve as a useful input into policy discussions on the medium-term economic recovery.

REFERENCES

ALVAREZ, F. E., D. ARGENTE, AND F. LIPPI (2020): "A Simple Planning Problem for COVID-19 Lockdown," NBER Working Paper 26981, https://doi.org/10.3386/w26981.

ATKESON, A. (2020): "What Will Be the Economic Impact of COVID-19 in the US? Rough Estimates of Disease Scenarios," NBER Working Paper 26867, https://doi.org/10.3386/w26867.

BARRO, R. J., J. F. URSÚA, AND J. WENG (2020): "The Coronavirus and the Great Influenza Pandemic: Lessons from the "Spanish Flu" for the Coronavirus's Potential Effects on Mortality and Economic Activity," NBER Working Paper 26866, https://doi.org/10.3386/w26866.

BERGER, D., K. HERKENHOFF, AND S. MONGEY (2020): "An SEIR Infectious Disease Model with Testing and Conditional Quarantine," Federal Reserve Bank of Minneapolis Working Paper 2020-17, https://doi.org/10.21034/sr.597.

BLANCHARD, O. AND J. GALÍ (2010): "Labor Markets and Monetary Policy: A New Keynesian Model with Unemployment," *American Economic Journal: Macroeconomics*, 2, 1–30, https://doi.org/10.1257/mac.2.2.1.

COLEMAN, II, W. J. (1991): "Equilibrium in a Production Economy with an Income Tax," *Econometrica*, 59, 1091–1104, https://doi.org/10.2307/2938175.

DEN HAAN, W. J., G. RAMEY, AND J. WATSON (2000): "Job Destruction and Propagation of Shocks," *American Economic Review*, 90, 482–498, https://doi.org/10.1257/aer.90.3.482.

EICHENBAUM, M. S., S. REBELO, AND M. TRABANDT (2020): "The Macroeconomics of Epidemics," NBER Working Paper 28882, https://doi.org/10.3386/w26882.

FARIA-E-CASTRO, M. (2020a): "Back-of-the-Envelope Estimates of Next Quarter's Unemployment Rate," Federal Reserve Bank of St. Louis On the Economy Blog.

——— (2020b): "Fiscal Policy during a Pandemic," Federal Reserve Bank of St. Louis Working Paper 2020-006, https://doi.org/10.20955/wp.2020.006.

FORNARO, L. AND M. WOLF (2020): "Covid-19 Coronavirus and Macroeconomic Policy," Barcelona Graduate School of Economics Working Paper 1169.

GARCIA, C. B. AND W. I. ZANGWILL (1981): *Pathways to Solutions, Fixed Points and Equilibria*, Prentice-Hall series in computational mathematics, Prentice-Hall.

GUERRIERI, V., G. LORENZONI, L. STRAUB, AND I. WERNING (2020): "Macroeconomic Implications of COVID-19: Can Negative Supply Shocks Cause Demand Shortages?" NBER Working Paper 26918, https://doi.org/10.3386/w26918.

HAGEDORN, M. AND I. MANOVSKII (2008): "The Cyclical Behavior of Equilibrium Unemployment and Vacancies Revisited," *American Economic Review*, 98, 1692–1706, https://doi.org/10.1257/aer.98.4.1692.

JONES, C. J., T. PHILIPPON, AND V. VENKATESWARAN (2020): "Optimal Mitigation Policies in a Pandemic: Social Distancing and Working from Home," NBER Working Paper 26984, https://doi.org/10.3386/w26984.

JORDÀ, O., S. R. SINGH, AND A. M. TAYLOR (2020): "Longer-run Economic Consequences of Pandemics," NBER Working Paper 26934, https://doi.org/10.3386/w26934.

JURADO, K., S. C. LUDVIGSON, AND S. NG (2015): "Measuring Uncertainty," *American Economic Review*, 105, 1177–1216, https://www.doi.org/10.1257/aer.20131193.

KOOP, G., M. H. PESARAN, AND S. M. POTTER (1996): "Impulse Response Analysis in Nonlinear Multivariate Models," *Journal of Econometrics*, 74, 119–147, https://doi.org/10.1016/0304-4076(95)01753-4.

KOPECKY, K. AND R. SUEN (2010): "Finite State Markov-chain Approximations to Highly Persistent Processes," *Review of Economic Dynamics*, 13, 701–714, https://doi.org/10.1016/j.red.2010.02.002.

PETROSKY-NADEAU, N. AND L. ZHANG (2017): "Solving the Diamond-Mortensen-Pissarides model accurately," *Quantitative Economics*, 8, 611–650, https://doi.org/10.3982/QE452.

PETROSKY-NADEAU, N., L. ZHANG, AND L.-A. KUEHN (2018): "Endogenous Disasters," *American Economic Review*, 108, 2212–2245, https://doi.org/10.1257/aer.20130025.

PIGUILLEM, F. AND L. SHI (2020): "The Optimal COVID-19 Quarantine and Testing Policies," EIEF Working Paper 2004.

PLANTE, M., A. W. RICHTER, AND N. A. THROCKMORTON (2018): "The Zero Lower Bound and Endogenous Uncertainty," *Economic Journal*, 128, 1730–1757, https://doi.org/10.1111/ecoj.12445.

RICHTER, A. W., N. A. THROCKMORTON, AND T. B. WALKER (2014): "Accuracy, Speed and Robustness of Policy Function Iteration," *Computational Economics*, 44, 445–476, https://doi.org/10.1007/s10614-013-9399-2.

ROUWENHORST, K. G. (1995): "Asset Pricing Implications of Equilibrium Business Cycle Models," in *Frontiers of Business Cycle Research*, ed. by T. F. Cooley, Princeton, NJ: Princeton University Press, 294–330.

SHIMER, R. (2005): "The Cyclical Behavior of Equilibrium Unemployment and Vacancies," *American Economic Review*, 95, 25–49, https://doi.org/10.1257/0002828053828572.

SIMS, C. A. (2002): "Solving Linear Rational Expectations Models," *Computational Economics*, 20, 1–20, https://doi.org/10.1023/A:1020517101123.

A PROOFS

Proof of Lemma 1 We insert our approximation for $\hat{q}_t$ into (17) to obtain

$$(\kappa/\bar{q})\exp(-\phi_{q,1}\hat{s}_t - \tfrac{1}{2}\phi_{q,2}\hat{s}_t^2) = 1 - b + \beta(\kappa/\bar{q})E_t[(1 - s_{t+1})\exp(-(\phi_{q,1}\hat{s}_{t+1} + \tfrac{1}{2}\phi_{q,2}\hat{s}_{t+1}^2))].$$

Substituting s_{t+1} with $\bar{s}\exp(\hat{s}_{t+1})$ yields

$$\begin{aligned}(\kappa/\bar{q})\exp(-\phi_{q,1}\hat{s}_t - \tfrac{1}{2}\phi_{q,2}\hat{s}_t^2) = 1 - b &+ \beta(\kappa/\bar{q})E_t[\exp(-(\phi_{q,1}\hat{s}_{t+1} + \tfrac{1}{2}\phi_{q,2}\hat{s}_{t+1}^2))] \\ &- \beta\bar{s}(\kappa/\bar{q})E_t[\exp(\hat{s}_{t+1} - (\phi_{q,1}\hat{s}_{t+1} + \tfrac{1}{2}\phi_{q,2}\hat{s}_{t+1}^2))].\end{aligned}$$

Now impose the separation rate process, $\hat{s}_{t+1} = \rho_s\hat{s}_t + \varepsilon_{s,t+1}$, to obtain

$$\begin{aligned}(\kappa/\bar{q})\exp(-\phi_{q,1}\hat{s}_t - \tfrac{1}{2}\phi_{q,2}\hat{s}_t^2) = 1 - b &\\ &+ \beta(\kappa/\bar{q})E_t[\exp(-\phi_{q,1}(\rho_s\hat{s}_t + \varepsilon_{s,t+1}) - \tfrac{1}{2}\phi_{q,2}(\rho_s\hat{s}_t + \varepsilon_{s,t+1})^2)] \\ &- \beta\bar{s}(\kappa/\bar{q})E_t[\exp((1 - \phi_{q,1})(\rho_s\hat{s}_t + \varepsilon_{s,t+1}) - \tfrac{1}{2}\phi_{q,2}(\rho_s\hat{s}_t + \varepsilon_{s,t+1})^2)].\end{aligned}$$

We can then simplify to obtain

$$\begin{aligned}\exp(-\phi_{q,1}\hat{s}_t - \tfrac{1}{2}\phi_{q,2}\hat{s}_t^2) &= \bar{q}(1 - b)/\kappa \\ &+ \beta E_t[\exp(-\phi_{q,1}(\rho_s\hat{s}_t + \varepsilon_{s,t+1}) - \tfrac{1}{2}\phi_{q,2}(\rho_s^2\hat{s}_t^2 + 2\rho_s\hat{s}_t\varepsilon_{s,t+1} + \varepsilon_{s,t+1}^2))] \\ &- \beta\bar{s}E_t[\exp((1 - \phi_{q,1})(\rho_s\hat{s}_t + \varepsilon_{s,t+1}) - \tfrac{1}{2}\phi_{q,2}(\rho_s^2\hat{s}_t^2 + 2\rho_s\hat{s}_t\varepsilon_{s,t+1} + \varepsilon_{s,t+1}^2))] \\ &= \bar{q}(1 - b)/\kappa \\ &+ \beta\exp(-\phi_{q,1}\rho_s\hat{s}_t - \tfrac{1}{2}\phi_{q,2}\rho_s^2\hat{s}_t^2) \\ &\times E_t[\exp(-(\phi_{q,1} + \phi_{q,2}\rho_s\hat{s}_t)\varepsilon_{s,t+1} - \tfrac{1}{2}\phi_{q,2}\varepsilon_{s,t+1}^2)] \\ &- \beta\bar{s}\exp(-\phi_{q,1}\rho_s\hat{s}_t - \tfrac{1}{2}\phi_{q,2}\rho_s^2\hat{s}_t^2)\exp(\rho_s\hat{s}_t) \\ &\times E_t[\exp((1 - \phi_{q,1} - \phi_{q,2}\rho_s\hat{s}_t)\varepsilon_{s,t+1} - \tfrac{1}{2}\phi_{q,2}\varepsilon_{s,t+1}^2)].\end{aligned}$$

To evaluate the expectations, note that if $\varepsilon_{t+1} \sim \mathbb{N}(0, \sigma^2)$, then

$$E_t[\exp(a\varepsilon_{t+1} - b\varepsilon_{t+1}^2)] = \exp(\tfrac{1}{2}\tfrac{a^2\sigma^2}{1+2b\sigma^2})\tfrac{1}{\sqrt{1+2b\sigma^2}}.$$

Applying this result implies

$$\begin{aligned}\exp(-(\phi_{q,1}\hat{s}_t + \tfrac{1}{2}\phi_{q,2}\hat{s}_t^2)) &= \bar{q}(1 - b)/\kappa \\ &+ \beta\exp(-\phi_{q,1}\rho_s\hat{s}_t - \tfrac{1}{2}\phi_{q,2}\rho_s^2\hat{s}_t^2)\tfrac{1}{\sqrt{1+\phi_{q,2}\sigma_s^2}}\exp(\tfrac{1}{2}\tfrac{(\phi_{q,1}+\phi_{q,2}\rho_s\hat{s}_t)^2\sigma_s^2}{1+\phi_{q,2}\sigma_s^2}) \\ &- \beta\bar{s}\exp(-\phi_{q,1}\rho_s\hat{s}_t - \tfrac{1}{2}\phi_{q,2}\rho_s^2\hat{s}_t^2)\tfrac{1}{\sqrt{1+\phi_{q,2}\sigma_s^2}}\exp(\rho_s\hat{s}_t) \\ &\times \exp(\tfrac{1}{2}\tfrac{(1-\phi_{q,1}-\phi_{q,2}\rho_s\hat{s}_t)^2\sigma_s^2}{1+\phi_{q,2}\sigma_s^2}).\end{aligned}$$

To ensure that the approximation is valid, we apply the limit as $\sigma_s \to 0$ to obtain

$$\exp(-(\phi_{q,1}\hat{s}_t + \tfrac{1}{2}\phi_{q,2}\hat{s}_t^2)) = \bar{q}(1-b)/\kappa + \beta\exp(-\phi_{q,1}\rho_s\hat{s}_t - \tfrac{1}{2}\phi_{q,2}\rho_s^2\hat{s}_t^2)(1-\bar{s}\exp(\rho_s\hat{s}_t)),$$

which is an identity in $\hat{s}_t$. To solve for the coefficients $\phi_{q,1}$ and $\phi_{q,2}$, we twice differentiate the identity with respect to $\hat{s}$. The left-hand side has first and second derivatives given by

$$-(\phi_{q,1} + \phi_{q,2}\hat{s}_t)\exp(-(\phi_{q,1}\hat{s}_t + \tfrac{1}{2}\phi_{q,2}\hat{s}_t^2))$$

and

$$-\phi_{q,2}\exp(-(\phi_{q,1}\hat{s}_t + \tfrac{1}{2}\phi_{q,2}\hat{s}_t^2))\frac{\bar{\kappa}}{\bar{q}} + (\phi_{q,1} + \phi_{q,2}\hat{s}_t)^2\exp(-(\phi_{q,1}\hat{s}_t + \tfrac{1}{2}\phi_{q,2}\hat{s}_t^2)).$$

When evaluated at $\hat{s}_t = 0$, these expressions become

$$-\phi_{q,1} \qquad \text{and} \qquad -\phi_{q,2} + \phi_{q,1}^2.$$

The right-hand side has derivatives

$$\begin{aligned}
&\beta(-\phi_{q,1}\rho_s - \phi_{q,2}\rho_s^2\hat{s}_t)\exp(-\phi_{q,1}\rho_s\hat{s}_t - \tfrac{1}{2}\phi_{q,2}\rho_s^2\hat{s}_t^2)\\
&-\beta\bar{s}((1-\phi_{q,1})\rho_s - \phi_{q,2}\rho_s^2\hat{s}_t)\exp((1-\phi_{q,1})\rho_s\hat{s}_t - \tfrac{1}{2}\phi_{q,2}\rho_s^2\hat{s}_t^2)
\end{aligned}$$

and

$$\begin{aligned}
&\beta(-\phi_{q,2}\rho_s^2)\exp(-\phi_{q,1}\rho_s\hat{s}_t - \tfrac{1}{2}\phi_{q,2}\rho_s^2\hat{s}_t^2)\\
&+\beta(\phi_{q,1}\rho_s + \phi_{q,2}\rho_s^2\hat{s}_t)^2\exp(-\phi_{q,1}\rho_s\hat{s}_t - \tfrac{1}{2}\phi_{q,2}\rho_s^2\hat{s}_t^2)\\
&-\beta\bar{s}(-\phi_{q,2}\rho_s^2)\exp((1-\phi_{q,1})\rho_s\hat{s}_t - \tfrac{1}{2}\phi_{q,2}\rho_s^2\hat{s}_t^2)\\
&+\beta\bar{s}((1-\phi_{q,1})\rho_s - \phi_{q,2}\rho_s^2\hat{s}_t)^2\exp((1-\phi_{q,1})\rho_s\hat{s}_t - \tfrac{1}{2}\phi_{q,2}\rho_s^2\hat{s}_t^2).
\end{aligned}$$

When evaluated at $\hat{s}_t = 0$, these expressions become

$$-\beta\phi_{q,1}\rho_s - \beta\bar{s}((1-\phi_{q,1})\rho_s)$$

and

$$\beta(-\phi_{q,2}\rho_s^2) + \beta(\phi_{q,1}\rho_s)^2 - \beta\bar{s}(-\phi_{q,2}\rho_s^2) - \beta\bar{s}((1-\phi_{q,1})\rho_s)^2.$$

Equating the left-hand and right-hand sides for the first and second derivatives yields

$$\begin{aligned}
\phi_{q,1} &= \frac{\beta\rho_s\bar{s}}{1-\beta\rho_s(1-\bar{s})} > 0,\\
\phi_{q,2} &= \frac{\beta\rho_s^2\bar{s}}{1-\beta\rho_s^2(1-\bar{s})}\frac{\beta\bar{s}(1-\beta\rho_s^2) + (1-\beta\rho_s)^2}{(1-\beta\rho_s(1-\bar{s}))^2} > 0.
\end{aligned}$$

Hence $\hat{q}_t$ is increasing and convex in the separation rate.

Proof of Proposition 1 Recall $mc_t = \kappa/q_t$. Taking natural logs of (18) yields

$$\ln v_t = \tfrac{1}{\iota}\ln(\kappa^{-\iota} mc_t^{\iota} - 1) + \ln(1 - (1 - s_t)n_{t-1}).$$

Define $\tilde{mc} \equiv \kappa^{-\iota}\bar{mc}^{\iota}$ and $\tilde{n} \equiv 1 - \bar{n} + \bar{s}\bar{n}$. Then apply a second order Taylor expansion to obtain

$$\tfrac{1}{\iota}\ln(\kappa^{-\iota} mc_t^{\iota} - 1) \approx \tfrac{1}{\iota}\ln(\tilde{mc} - 1) + \tfrac{\tilde{mc}}{\tilde{mc}-1}\hat{\kappa}_t - \tfrac{1}{2}\tfrac{\iota\tilde{mc}}{(\tilde{mc}-1)^2}\hat{\kappa}_t^2$$

and

$$\begin{aligned}\ln(1 - n_{t-1} + s_t n_{t-1}) \approx \ln\tilde{n} + \tfrac{\bar{s}\bar{n}}{\tilde{n}}(\hat{s}_t + \tfrac{1}{2}\hat{s}_t^2) - \tfrac{1}{2}\tfrac{\bar{s}^2\bar{n}^2}{\tilde{n}^2}\hat{s}_t^2 \\ - \tfrac{\bar{n}(1-\bar{s})}{\tilde{n}}(\hat{n}_{t-1} + \tfrac{1}{2}\hat{n}_{t-1}^2) + \tfrac{1}{2}\tfrac{\bar{n}^2(1-\bar{s})^2}{\tilde{n}^2}\hat{n}_{t-1}^2 + \tfrac{\bar{s}\bar{n}}{\tilde{n}^2}\hat{s}_t\hat{n}_{t-1}.\end{aligned}$$

Combining the previous two approximations then yields

$$\begin{aligned}\hat{v}_t = (\tfrac{\bar{s}\bar{n}}{\tilde{n}}(1 + \tfrac{1}{\tilde{n}}\hat{n}_{t-1}) - \tfrac{\tilde{mc}}{\tilde{mc}-1}\phi_{q,1})\hat{s}_t + \tfrac{1}{2}(\tfrac{\bar{s}\bar{n}(1-\bar{n})}{\tilde{n}^2} - \tfrac{\tilde{mc}}{\tilde{mc}-1}(\phi_{q,2} + \tfrac{\iota}{\tilde{mc}-1}\phi_{q,1}^2))\hat{s}_t^2 \\ - \tfrac{\bar{n}(1-\bar{s})}{\tilde{n}}\hat{n}_{t-1} + \tfrac{\bar{n}(1-\bar{s})}{2}\tfrac{2\bar{n}(1-\bar{s})-1}{\tilde{n}^2}\hat{n}_{t-1}^2.\end{aligned}$$

To simplify the expressions, we make use of the following deterministic steady-state relations:

$$\begin{aligned}\bar{\theta} = (1 - \bar{q}^{\iota})^{1/\iota}/\bar{q}, \quad \bar{f} = (1 - \bar{q}^{\iota})^{1/\iota}, \quad \bar{n} = \bar{q}\bar{\theta}/(\bar{s} + \bar{q}\bar{\theta}(1 - \bar{s})), \\ \bar{u} = \bar{s}(1 - \bar{q}\bar{\theta})/(\bar{s} + \bar{q}\bar{\theta}(1 - \bar{s})), \quad \bar{u}^s = \bar{s}/(\bar{s} + \bar{f}(1 - \bar{s})), \quad \bar{f} = \bar{s}\bar{n}/\bar{u}^s.\end{aligned}$$

Using these conditions, we obtain

$$\hat{v}_t = \phi_{v,1}(\hat{n}_{t-1})\hat{s}_t + \tfrac{1}{2}\phi_{v,2}\hat{s}_t^2 + \psi_{v,1}\hat{n}_{t-1} + \tfrac{1}{2}\psi_{v,2}\hat{n}_{t-1}^2,$$

where

$$\begin{aligned}\phi_{v,1} &= \bar{f}(1 + \hat{n}_{t-1}/\bar{u}^s) - \phi_{q,1}/(1 - \bar{q}^{\iota}) \\ \phi_{v,2} &= \bar{f}(1 - \bar{f}) - ((1 - \bar{q}^{\iota})\phi_{q,2} + \bar{q}^{\iota}\iota\phi_{q,1}^2)/(1 - \bar{q}^{\iota})^2 \\ \psi_{v,1} &= -\bar{n}(1 - \bar{s})/\bar{u}^s \\ \psi_{v,2} &= \bar{n}(1 - \bar{s})(2\bar{n}(1 - \bar{s}) - 1)/(\bar{u}^s)^2\end{aligned}$$

Proof of Lemma 2 First note $u_t = 1 - n_t$, so it is sufficient to focus on employment:

$$n_t = n(s_t, n_{t-1}) = (1 - s_t)n_{t-1} + q_t v_t.$$

Using second order Taylor expansions, we obtain

$$(1 - s_t)n_{t-1} \approx (1 - \bar{s})\bar{n} + (1 - \bar{s})\bar{n}(\hat{n}_{t-1} + \tfrac{1}{2}\hat{n}_{t-1}^2) - \bar{s}\bar{n}(\hat{s}_t + \tfrac{1}{2}\hat{s}_t^2)$$

and

$$q_t v_t \approx \bar{q}\bar{v} + \bar{q}\bar{v}(\hat{v}_t + \tfrac{1}{2}\hat{v}_t^2) + \bar{q}\bar{v}(\hat{q}_t + \tfrac{1}{2}\hat{q}_t^2).$$

Combining the previous two approximations then yields

$$n_t \approx (1-\bar{s})\bar{n} + (1-\bar{s})\bar{n}(\hat{n}_{t-1} + \tfrac{1}{2}\hat{n}_{t-1}^2) - \bar{s}\bar{n}(\hat{s}_t + \tfrac{1}{2}\hat{s}_t^2) + \bar{q}\bar{v} + \bar{q}\bar{v}(\hat{v}_t + \tfrac{1}{2}\hat{v}_t^2) + \bar{q}\bar{v}(\hat{q}_t + \tfrac{1}{2}\hat{q}_t^2).$$

Using Lemma 1 and Proposition 1, this simplifies to

$$\begin{aligned} n_t \approx\ & (1-\bar{s})\bar{n} + \bar{q}\bar{v} + \bar{q}\bar{v}(\phi_{q,1} + \phi_{v,1} - 1 + (\phi_{q,2} + \phi_{q,1}^2 + \phi_{v,2} + \phi_{v,1}^2 - 1)\rho_s\hat{s}_{t-1})\sigma_s\varepsilon_{s,t} \\ & + \bar{q}\bar{v}(\phi_{q,1} + \phi_{v,1} - 1)\rho_s\hat{s}_{t-1} + \tfrac{1}{2}\bar{q}\bar{v}(\phi_{q,2} + \phi_{q,1}^2 + \phi_{v,2} + \phi_{v,1}^2 - 1)\rho_s^2\hat{s}_{t-1}^2 \\ & + \tfrac{1}{2}\bar{q}\bar{v}(\phi_{q,2} + \phi_{q,1}^2 + \phi_{v,2} + \phi_{v,1}^2 - 1)\sigma_s^2\varepsilon_{s,t}^2 + ((1-\bar{s})\bar{n} - \bar{q}\bar{v}\psi_{v,1})\hat{n}_{t-1} \\ & + \tfrac{1}{2}((1-\bar{s})\bar{n} + \bar{q}\bar{v}(\psi_{v,2} + \psi_{v,1}^2))\hat{n}_{t-1}^2. \end{aligned}$$

The variance of n_t, conditional on period $t-1$ information and up to a second order is given by

$$\mathrm{Var}_{t-1}(n_t) \approx (\bar{q}\bar{v}(\phi_{q,1} + \phi_{v,1} - 1 + (\phi_{q,2} + \phi_{q,1}^2 + \phi_{v,2} + \phi_{v,1}^2 - 1)\rho_s\hat{s}_{t-1}))^2\sigma_s^2.$$

Since $\mathrm{Var}_{t-1}(u_t) = \mathrm{Var}_{t-1}(n_t)$, we obtain

$$\mathcal{U}_{t,t+1}^u = (\bar{q}\bar{v}(\phi_{q,1} + \phi_{v,1}(\hat{n}_{t-1}) - 1 + (\phi_{q,2} + \phi_{q,1}^2 + \phi_{v,2} + \phi_{v,1}(\hat{n}_{t-1})^2 - 1)\rho_s\hat{s}_t))\sigma_s.$$

Proof of Proposition 2 Using Lemma 2 implies

$$\mathcal{U}_{t,t+1}^u / d\hat{s}_t = \bar{q}\bar{v}(\phi_{q,2} + \phi_{q,1}^2 + \phi_{v,2} + \phi_{v,1}(\hat{n}_{t-1})^2 - 1)\rho_s\sigma_s^2.$$

B SOLUTION METHODS

Nonlinear Solution We begin by writing the equilibrium system as $E[g(\mathbf{x}_{t+1}, \mathbf{x}_t, \varepsilon_{t+1})|\mathbf{z}_t, \vartheta] = 0$, where g is a vector-valued function, $\mathbf{x}_t$ is a vector of variables, ε_t is a vector of shocks, $\mathbf{z}_t$ is a vector of states, and ϑ is a vector of parameters. There are many ways to discretize the exogenous state, s_t. We use the Markov chain in Rouwenhorst (1995), which Kopecky and Suen (2010) show outperforms other methods for approximating autoregressive processes. The bounds on the endogenous state variable, n_{t-1}, are set to $[-50\%, +6\%]$ of the deterministic steady-state value, $\bar{n}$, which contain at least 99% of the ergodic distribution and minimize extrapolation for the COVID-19 separation rate shock simulations. We discretize the n_{t-1} and s_t into 101 and 11 evenly-spaced points, respectively. The product of the points in each dimension, D, represents the total nodes in the state space ($D = 1{,}111$). The realization of $\mathbf{z}_t$ on node d is denoted $\mathbf{z}_t(d)$. The Rouwenhorst method provides integration nodes, $[s_{t+1}(m)]$, with weights, $\phi(m)$, for $m \in \{1, \ldots, M\}$. Since the separation

rate evolves according to a Markov chain, the number of realizations of s_{t+1} is the same as s_t (11).

Since vacancies $v_t \geq 0$, we introduce an auxiliary variable, μ_t, such that $v_t = \max\{0, \mu_t\}^2$ and $\lambda_t = \max\{0, -\mu_t\}^2$, where λ_t is the Lagrange multiplier on the non-negativity constraint. If $\mu_t \geq 0$, then $v_t = \mu_t^2$ and $\lambda_t = 0$. When $\mu_t < 0$, the constraint is binding, $v_t = 0$, and $\lambda_t = \mu_t^2$. Therefore, the constraint on v_t is transformed into a pair of equalities (Garcia and Zangwill, 1981).

The vector of policy functions and the realization on node d are denoted $\mathbf{pf}_t$ and $\mathbf{pf}_t(d)$, where $\mathbf{pf}_t \equiv \mu_t(\mathbf{z}_t)$. The following steps outline our policy function iteration algorithm:

1. Use Sims's (2002) `gensys` algorithm to solve the log-linear model. Then map the solution for the policy functions to the discretized state space. This provides an initial conjecture.

2. On iteration $j \in \{1, 2, \ldots\}$ and each node $d \in \{1, \ldots, D\}$, use Chris Sims's `csolve` to find $\mathbf{pf}_t(d)$ to satisfy $E[g(\cdot)|\mathbf{z}_t(d), \vartheta] \approx 0$. Guess $\mathbf{pf}_t(d) = \mathbf{pf}_{j-1}(d)$. Then apply the following:
   (a) Solve for all variables dated at time t, given $\mathbf{pf}_t(d)$ and $\mathbf{z}_t(d)$.
   (b) Linearly interpolate the policy functions, $\mathbf{pf}_{j-1}$, at the updated state variables, $\mathbf{z}_{t+1}(m)$, to obtain $\mathbf{pf}_{t+1}(m)$ on every integration node, $m \in \{1, \ldots, M\}$.
   (c) Given $\{\mathbf{pf}_{t+1}(m)\}_{m=1}^M$, solve for the other elements of $\mathbf{s}_{t+1}(m)$ and compute

$$E[g(\mathbf{x}_{t+1}, \mathbf{x}_t(d), \varepsilon_{t+1})|\mathbf{z}_t(d), \vartheta] \approx \textstyle\sum_{m=1}^M \phi(m) g(\mathbf{x}_{t+1}(m), \mathbf{x}_t(d), \varepsilon_{t+1}(m)).$$

   When `csolve` converges, set $\mathbf{pf}_j(d) = \mathbf{pf}_t(d)$.

3. Repeat step 2 until $\text{maxdist}_j < 10^{-8}$, where $\text{maxdist}_j \equiv \max\{|\mathbf{pf}_j - \mathbf{pf}_{j-1}|\}$. When that criterion is satisfied, the algorithm has converged to an approximate nonlinear solution.

Linear Solution We solve the following log-linear equilibrium system according to Sims (2002):

$$\begin{gathered}
\hat{v}_t = 2\hat{\mu}_t, \\
\hat{n}_t = (1-\bar{s})\hat{n}_{t-1} - \bar{s}\hat{s}_t + \bar{s}(\hat{q}_t + \hat{v}_t), \\
\hat{\theta}_t = \hat{v}_t - \hat{u}_t^s, \\
\bar{u}^s \hat{u}_t^s = \bar{s}\bar{n}\hat{s}_t - (1-\bar{s})\bar{n}\hat{n}_{t-1}, \\
\bar{u}\hat{u}_t + \bar{n}\hat{n}_t = 0, \\
\bar{c}\hat{c}_t + \kappa\bar{v}\hat{v}_t = \bar{n}\hat{n}_t, \\
\hat{q}_t = -\bar{\theta}^\iota \hat{\theta}_t/(1+\bar{\theta}^\iota), \\
\bar{w}\hat{w}_t = \beta\eta\kappa(1-\bar{s})\bar{\theta}(E_t\hat{\theta}_{t+1} - \bar{s}E_t\hat{s}_{t+1}/(1-\bar{s})), \\
(\kappa/\bar{q})\hat{q}_t = \bar{w}\hat{w}_t + \beta(1-\bar{s})(\kappa/\bar{q})(E_t\hat{q}_{t+1} + \bar{s}E_t\hat{s}_{t+1}/(1-\bar{s})), \\
\hat{s}_t = \rho_s\hat{s}_{t-1} + \sigma_s\varepsilon_{s,t+1}.
\end{gathered}$$